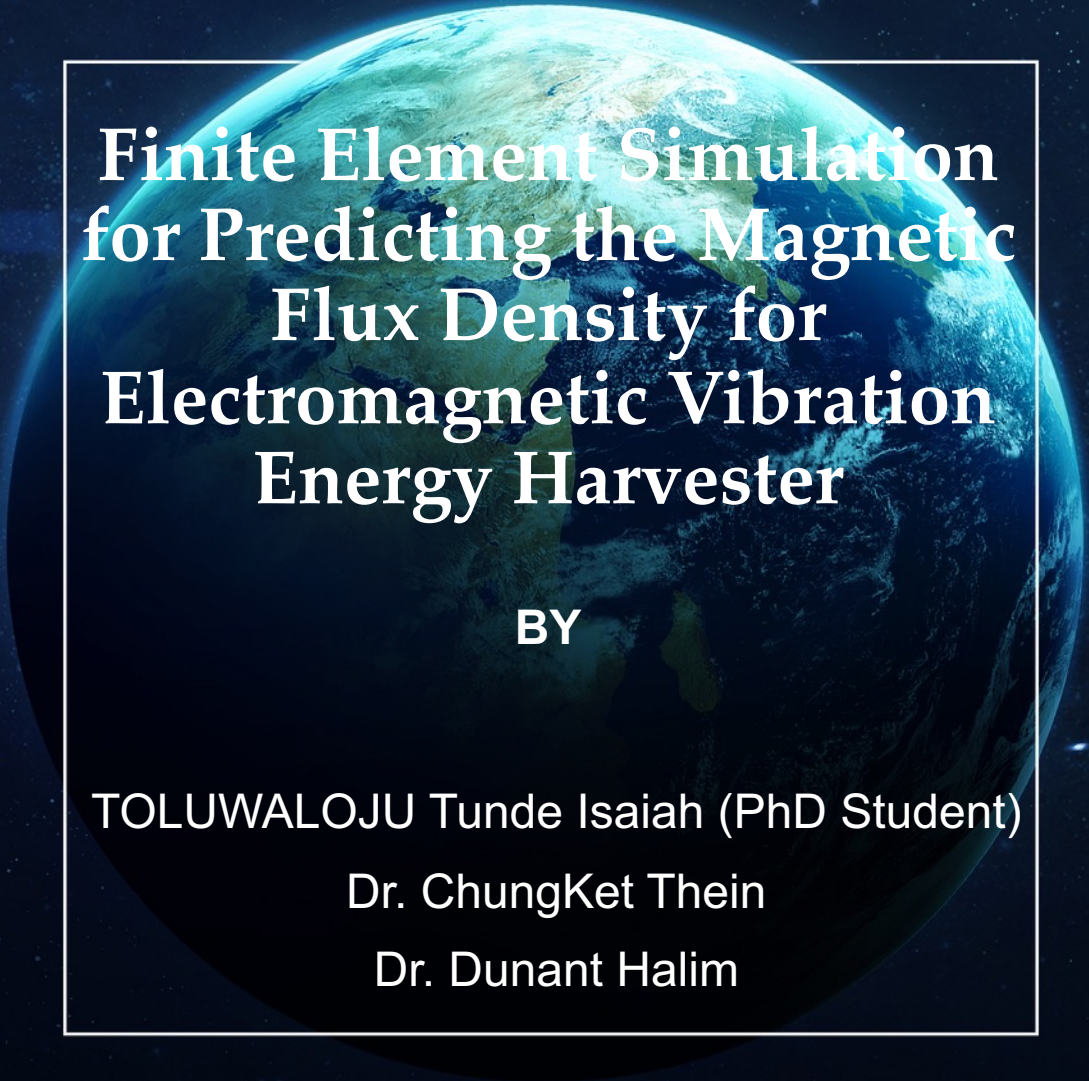




University of
Nottingham

UK | CHINA | MALAYSIA

A large, glowing blue and green Earth is centered in the background, set against a dark space with scattered stars. A white rectangular border frames the central text.

Finite Element Simulation for Predicting the Magnetic Flux Density for Electromagnetic Vibration Energy Harvester

BY

TOLUWALOJU Tunde Isaiah (PhD Student)

Dr. ChungKet Thein

Dr. Dunant Halim





Table Of Content

- Introduction
- Aims/Objectives Design Model.
- Harvester Model
- Governing Equation
- FEMM Simulation and Modified Coupling Equations.
- Results
- Conclusion





Introduction



- A vibration energy harvester (VEH) has proven worthy of having the capacity to sustainably supply electrical power to wireless sensor nodes (WSN's) and body sensor networks (bodyNET) [1]
- Fig. 1 shows a summary of different optimization paths to realize better performance of a VEH.

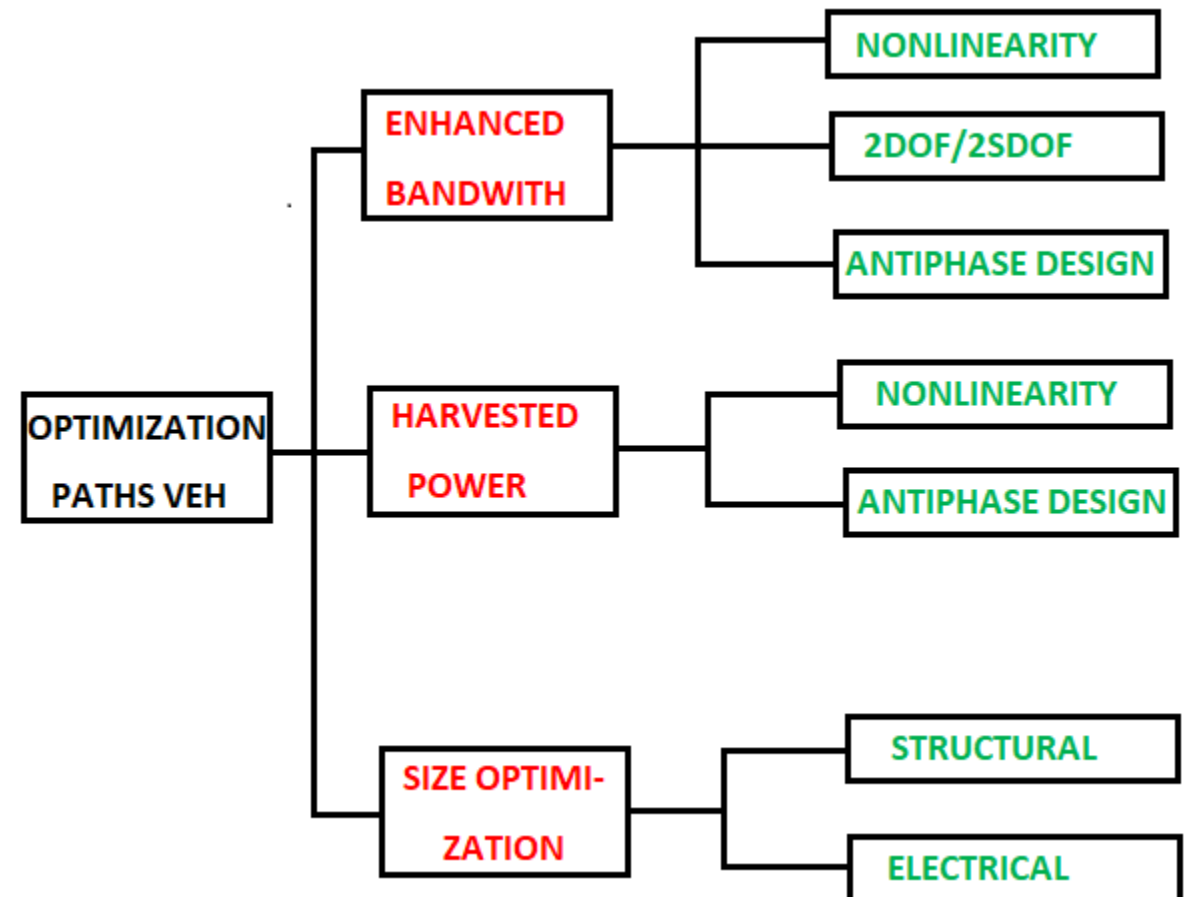


Figure. 1 Optimization paths in VEH



Aims/Objectives and Design Model

- This paper focuses on realizing an approach to ensure an accurate prediction of the optimum overall size that will maximize the coupling coefficient and power output on the electromagnetic transducer of a VEH.
- Fig. 2. shows the general geometry and model that was employed to fully characterize the transduction iron-magnet-coil that will be modelled in the FEMM software.

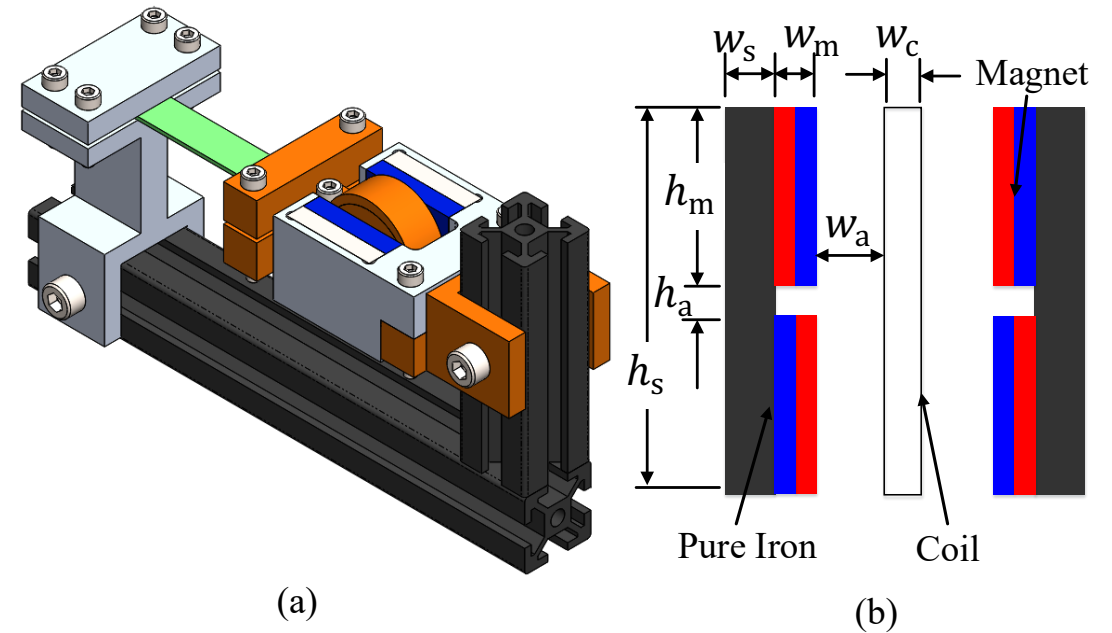


Figure 2. (a) SDOF cantilevered electromagnetic vibration energy harvester and (b) model geometry for the iron-magnet-coil part.



Governing Equations



- During excitation, the magnetic flux of the permanent magnet couples into the freely oscillating coil, hence, voltages are induced in the coil according to the principle of electromagnetic induction. K is defined as the degree of coupling was obtained [9].

$$K = NBl_c c_f \quad (1)$$

where N, B, l_c and c_f are effective turn, flux density, effective length and coil fill factor.

- Eq. (1) premised a caution for careful alignment of the coil in the magnet because zero flux coupling into the coil implies an approximately zero voltage is induced in the coil.



Governing Equations



- From the Maxwell theory

$$\nabla \cdot (\mu H) = 0 \quad (2)$$

$$\nabla \times (\mu H) = \mu_0 J \quad (3)$$

where $B = \mu H$, J and H are the magnetic flux, current and magnetic field densities, μ is permeability of the magnetic material.

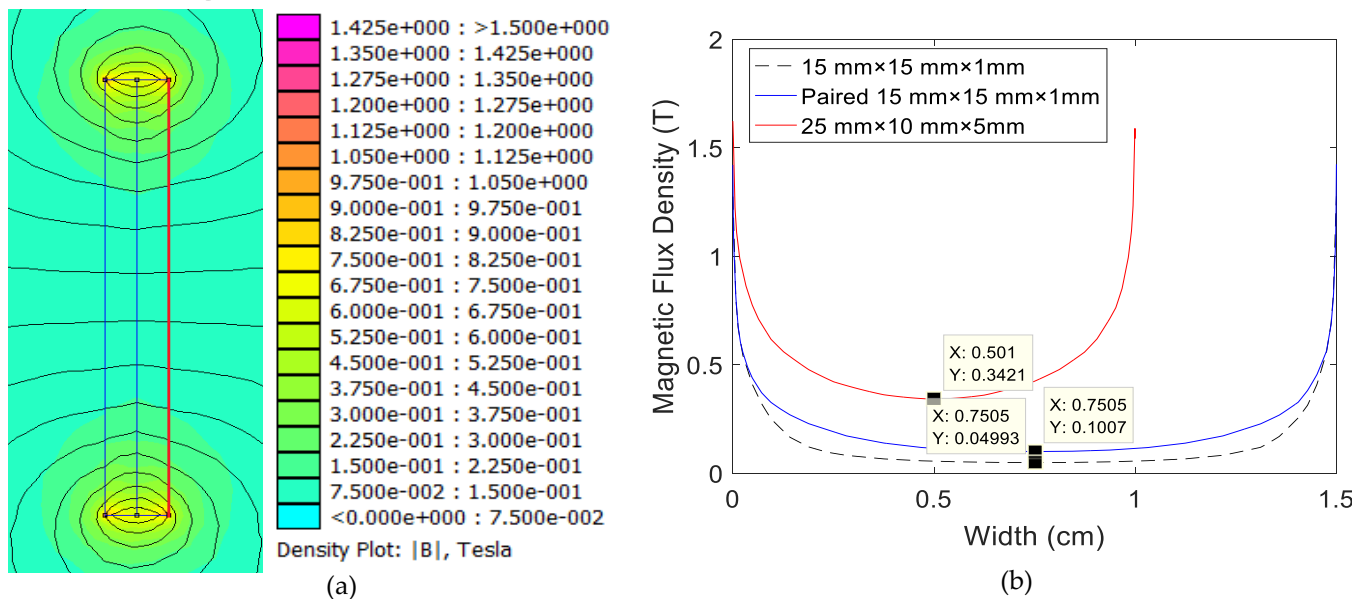
- Eqs. (2) and (3) implies that magnet has no isolated magnetic poles and that circulating magnetic fields are produced by changing the electric current. Eq. 3 is trivial in the absence of charged particles.
- In the eventuality of using more than one magnet, Eq. (2) also sets an order for which the transduction magnet must be aligned.



FEMM Simulation and Modified Coupling Equations



- FEMM predicted average magnetic flux density of 0.04993 T and 0.1007 T at the center of the single and paired magnets respectively as shown in Fig. 2(b) while Fig. 2(a) shows the FEMM pattern on the paired magnet.



The predicted B values realized a flux density per unit volume (β) as.

Magnet Configuration	$\beta (T\text{mm}^{-3})$
25mm×10 mm×5 mm	2.740×10^{-4}
15 mm×15 mm×1 mm paired	2.234×10^{-4}
15 mm×15 mm×1 mm single	2.210×10^{-4}

Figure 2. (a) Flux density pattern from FEMM of 15 mm × 15 mm × 1 mm (paired) and (b) flux density line plot for different magnet models.



FEMM Simulation and Modified Coupling Equations

- A line of fit and fit equation between B and the coil thickness measured in millimeters (w_c) was obtained as shown in Eq. (7).

$$B = -0.166 \ln w_c + 0.6357 \quad (7)$$

- From Eqs. (1), (7) and (8) an empirical relation between the magnet flux density per unit volume of the transduction coil was obtained as

$$\bar{\beta} = (1/\bar{v})(-0.166 \ln w_c + 0.6357) \quad (8)$$

- Eqs. (8) and (6) are sufficient to make a prediction of the flux density per volume of a coil and the coupling coefficient on any coil geometry, respectively.





Results



- Table 1 shows a summary of the flux density B and leakage sufficient iron cladding thickness over different coil width (w_c)

Model	w_c (mm)	w_s (mm)	w_T (mm)	N_{c-2}	B (T)	$\bar{\beta}$ ($T\text{mm}^{-3}$)	K ($T\text{mm}$)
1	1.00	5.50	19.00	$\mu_1 N_{c-2}$	0.6226	$0.6226/(\mu_1 \bar{v}_{c-2})$	$0.5663\mu_1 l_c N_{c-2}$
2	2.00	5.20	19.40	$\mu_2 N_{c-2}$	0.5450	$0.5450/(\mu_2 \bar{v}_{c-2})$	$0.4957\mu_2 l_c N_{c-2}$
3	4.00	3.70	18.40	$\mu_3 N_{c-2}$	0.4373	$0.4373/(\mu_3 \bar{v}_{c-2})$	$0.3978\mu_3 l_c N_{c-2}$
4	6.00	3.53	20.06	$\mu_4 N_{c-2}$	0.3438	$0.3438/(\mu_4 \bar{v}_{c-2})$	$0.3127\mu_4 l_c N_{c-2}$
5	8.00	3.60	22.20	$\mu_5 N_{c-2}$	0.2955	$0.2955/(\mu_5 \bar{v}_{c-2})$	$0.2688\mu_5 l_c N_{c-2}$
6	10.00	3.56	24.00	$\mu_6 N_{c-2}$	0.2562	$0.2562/(\mu_6 \bar{v}_{c-2})$	$0.2331\mu_6 l_c N_{c-2}$
7	12.00	4.00	27.00	$\mu_7 N_{c-2}$	0.2267	$0.2267/(\mu_7 \bar{v}_{c-2})$	$0.2062\mu_7 l_c N_{c-2}$

- The table shows dependency of $\bar{\beta}$ and K for any coil on width ratio μ_i , effective length (l_c) and coil turn (N_{c-2}) of the reference coil.



Results



- Fig. 3 shows the result from the FEMM simulation. The location of the coil corresponding to each simulation is outlined in thick red lines.

- The dotted green line in Fig. 4 shows the level of flux at which the harvesters become size (thickness) optimized in term of the flux density (B) and degree of coupling (K).

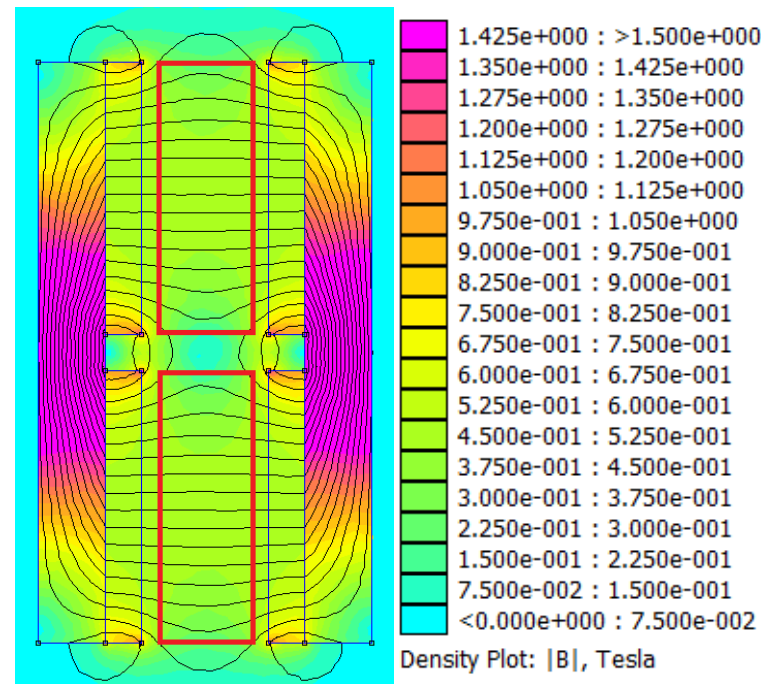


Figure 3. Magnet-coil simulation output on FEMM for 4 mm coil width.

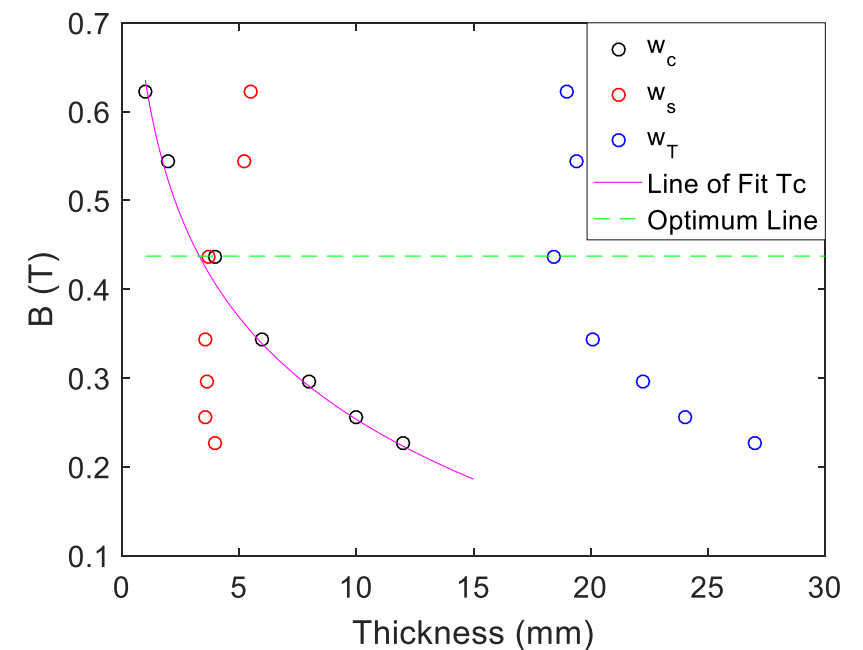


Figure 4. Variation of B with geometry thicknesses.



Conclusion

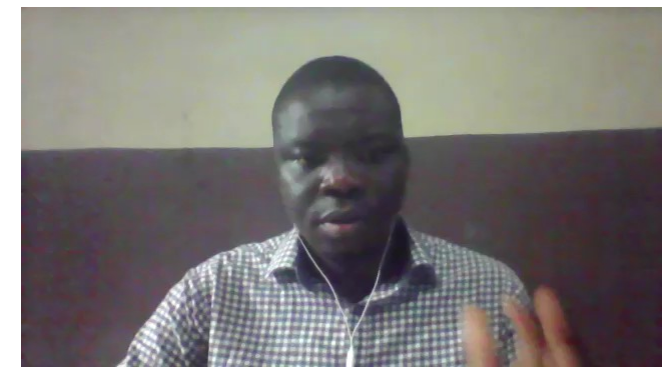
- From the forgone discussions and analysis, the following conclusions was reached among others
 - i. A nonlinear relationship existed between K and β . Both were respectively optimized at $0.3978\mu_3 l_c N_{c-2}$ Tmm and $0.4373 / (\mu_3 \bar{v}_{c-2}) \text{Tmm}^{-3}$.
 - ii. Given any coil of known volume, it is possible to make a relatively accurate prediction of the magnetic flux density using Eq. (10) when such coil is placed in the field of permanent magnet that are paired and arranged as shown in Fig. 1





References

- [1] T. He, X. Guo, and C. Lee, "Flourishing energy harvesters for future body sensor network : from single to multiple energy sources," *ISCIENCE*, vol. 24, no. 1, p. 101934, 2021.
- [2] T. I. Toluwalaju, C. K. Thein, and D. Halim, "An Effect of Coupling Factor on the Power Output for Electromagnetic Vibration Energy Harvester," *Eng. Proc.*, vol. 10, no. 1, p. 5, 2021.





University of
Nottingham

UK | CHINA | MALAYSIA

Thank You.

